Integral representation for scattering phase shifts via the phase-amplitude approach

D. Shu, I. Simbotin, and R. Côté

Phys. Rev. A **97**, 022701 — Published 1 February 2018

DOI: 10.1103/PhysRevA.97.022701

Integral representation for scattering phase shifts via the phase–amplitude approach

D. Shu, I. Simbotin, and R. Côté
Department of Physics, University of Connecticut, 2152 Hillside Rd., Storrs, CT 06269-3046, USA
(Dated: January 16, 2018)

A novel integral representation for scattering phase shifts is obtained based on a modified version of Milne's phase–amplitude approach [W. E. Milne, Phys. Rev. **35**, 863 (1930)]. We replace Milne's nonlinear differential equation for the amplitude function y with an equivalent linear equation for the envelope $\rho = y^2$, which renders the integral representations highly amenable to numerical implementations. The phase shift is obtained directly from Milne's phase function, which in turn is expressed in terms of the envelope function. We illustrate the advantages of the new representation with two scattering potentials. The integral representation presented in this work is fully general and it can be used for any type of scattering potential, including the Coulomb potential.

I. INTRODUCTION

The phase–amplitude approach for Schrödinger's radial (or one-dimensional) equation was pioneered by Milne [1], and has since been used extensively in atomic and molecular physics [2–14], in chemical physics [15–17], and in other areas of physics [18–28]. Although it was originally intended for tackling bound states, the phase–amplitude method is also applicable for scattering problems; indeed, Milne's approach is especially suitable in the framework of many-channel quantum defect theory [29–32] because it makes it possible to construct optimal reference functions in each scattering channel.

The virtues of Milne's approach stem from the fact that phases and amplitudes are quantities which are well behaved in the energy domain, even across channel thresholds. Moreover, the phase–amplitude method allows for highly efficient numerical implementations, because the direct computation of highly oscillatory wave functions can be avoided entirely; instead, any solution of the radial equation is evaluated accurately in terms of the amplitude and phase functions, which have a simple radial dependence.

In this work we use a modified version of Milne's method to derive a novel integral representation which yields the true value of the scattering phase shift, despite the modulo π ambiguity inherent in its usual definition. We apply our new approach to scattering potentials with long-range inverse power-law behaviors, which commonly appear in atomic, molecular, and optical physics, such as in our previous studies of R^{-3} atom–wall interactions [33, 34], excited electronic states in homonuclear molecules [35], or anisotropic dipolar interactions [36], the R^{-4} potential in atom–ion collisions [37], or R^{-5} between two Rydberg atoms in specific states [38, 39], the R^{-6} van der Waals interactions between atoms [40–42], and the inverse quadratic interaction appearing in Efimov physics [43]. We begin with a simple integral representation in Sec. II A, which we generalize for the Coulomb case in Sec. II B. We give a brief discussion of envelope and phase functions in Sec. II C, with additional details of the phase–amplitude approach presented in the Appendix. In Sec. II D we derive a two-envelope formula for phase shifts, which is essential for high partial waves. The computational approach is discussed in Sec. III, and we illustrate the usefulness of our integral representations with numerical applications in Sec. IV for R^{-1} and R^{-3} long-range potentials. Finally, we give concluding remarks in Sec. V. Technical details and derivations are also given in the Appendices.

II. THEORY

We consider the radial Schrödinger equation for a spherically symmetric potential $V(R)$,

$$\psi'' = U\psi, \qquad U = 2\mu\big(V_{\rm eff} - E\big), \tag{1}$$

where $V_{\rm eff}(R) = V(R) + \frac{\ell(\ell+1)}{2\mu R^2}$ is the effective potential, μ is the reduced mass of the two particles undergoing scattering, and $E > 0$ is the energy in the center-of-mass frame. Atomic units are used throughout.

Assuming that the interaction potential $V(R)$ vanishes faster than R^{-1} asymptotically, the physical solution $\psi(R)$ has the well known asymptotic behavior

$$\psi(R) \xrightarrow{R\to\infty} \sin(kR - \ell\tfrac{\pi}{2} + \delta_\ell), \tag{2}$$

which yields the scattering phase shift δ_ℓ for partial wave ℓ. In the equation above, $k = \sqrt{2\mu E}$ is the momentum for the relative motion. The phase shift is usually obtained from the matching condition,

$$\psi(R) = Af(R) + Bg(R), \tag{3}$$

where f and g are exact solutions of the radial equation, specified by their asymptotic behavior,

$$f(R) \xrightarrow{R\to\infty} \sin(kR - \ell\tfrac{\pi}{2}) \tag{4}$$

$$g(R) \xrightarrow{R\to\infty} \cos(kR - \ell\tfrac{\pi}{2}). \tag{5}$$

From the equations above we have $\delta_\ell = \arctan(B/A)$, which yields the phase shift modulo π, i.e., $\delta_\ell \in [-\frac{\pi}{2}, \frac{\pi}{2}]$. To simplify our notation, we shall omit the label ℓ for ψ, f, g and other related quantities, except for the phase shift δ_ℓ.

A. Integral representation for the *full* phase shift

We now derive an expression for δ_ℓ which does not rely on the explicit evaluation of wave functions; instead, the phase shift will be extracted from an R-dependent phase function.

Our approach follows Milne's phase–amplitude method [1], which we review in appendices A, B, C. We emphasize that the *true* value of δ_ℓ will be obtained, despite the modulo π ambiguity inherent in its customary definition.

We first introduce the envelope function

$$\rho = f^2 + g^2, \tag{6}$$

with f and g exact solutions of the radial equation (1) obeying the asymptotic behavior (4, 5). The phase function θ is constructed by integrating

$$\theta' \equiv \frac{d\theta}{dR} = \frac{k}{\rho}. \tag{7}$$

We remark that $\theta(R)$ is defined up to an integration constant, which can be chosen freely; a judicious choice guided by the computational strategy shall be made in Sec. II C.

As shown by Milne [1], the general solution of the radial equation (1) can be represented exactly in terms of ρ and θ. In particular, the physical solution reads

$$\psi(R) = \sqrt{\rho(R)}\sin[\theta(R) - \theta(0)]. \tag{8}$$

Note that $\psi(R)$ vanishes explicitly at $R = 0$, while Eqs. (4, 5) ensure a very simple asymptotic behavior for ρ and θ,

$$\rho(R) \xrightarrow{R\to\infty} 1 \tag{9}$$

$$\theta(R) \xrightarrow{R\to\infty} kR + \text{const.} \tag{10}$$

We now define the reduced phase

$$\tilde{\theta}(R) \equiv \theta(R) - kR, \tag{11}$$

and use Eqs. (9, 10) to find the asymptotic behavior of Milne's parametrization (8),

$$\psi(R) \xrightarrow{R\to\infty} \sin[kR + \tilde{\theta}(\infty) - \theta(0)],$$

which is identical to the asymptotic behavior of ψ in Eq. (2). Consequently, we obtain

$$\delta_\ell - \ell\tfrac{\pi}{2} = \tilde{\theta}(\infty) - \theta(0). \tag{12}$$

Making use of Eq. (11) we have $\theta(0) = \tilde{\theta}(0)$, and Eqs. (7, 11) yield $\tilde{\theta}' = \frac{k}{\rho} - k$. Hence, Eq. (12) can be recast as an integral representation,

$$\begin{aligned}\delta_\ell - \ell\tfrac{\pi}{2} &= \tilde{\theta}(\infty) - \tilde{\theta}(0) \\ &= k\int_0^\infty dr\left[\frac{1}{\rho(r)} - 1\right].\end{aligned} \tag{13}$$

We remark that the reduced phase $\tilde{\theta}(R)$ defined in Eq. (11) cannot be regarded as the nontrivial phase contribution, as it also includes the Bessel contribution (due to the centrifugal term). Therefore, strictly speaking, the equation above yields the *full* phase shift ($\delta_\ell - \ell\frac{\pi}{2}$).

B. Generalization to potentials with a Coulomb term

So far, we assumed that the potential $V(R)$ vanishes faster than R^{-1} asymptotically. In this section we consider the general case when $V(R)$ contains a Coulomb term,

$$V_C(R) = \frac{Z_1 Z_2}{R}. \tag{14}$$

with $Z_{1,2}$ the electric charges of the two colliding particles. The remainder $(V - V_C)$ of the interaction potential is responsible for the phase shift δ_ℓ, which is obtained from the well known asymptotic behavior

$$\psi(R) \xrightarrow{R\to\infty} \sin\left[kR - \tfrac{C}{k}\ln(2kR) + \eta_\ell - \ell\tfrac{\pi}{2} + \delta_\ell\right], \tag{15}$$

where $\eta_\ell = \arg\Gamma(\ell + 1 + i\frac{C}{k})$ is the Coulomb phase shift [44], and $C \equiv \mu Z_1 Z_2$. Following the same steps as in the previous section, we use again Milne's parametrization (8) for the physical wave function, namely $\psi(R) = \sqrt{\rho(R)}\sin[\theta(R) - \theta(0)]$, with the phase θ behaving asymptotically as

$$\theta(R) \xrightarrow{R\to\infty} kR - \tfrac{C}{k}\ln(2kR) + \text{const}, \tag{16}$$

which is the generalized version of Eq. (10). Accordingly, the reduced phase is again defined such that it is finite asymptotically,

$$\tilde{\theta}(R) \equiv \theta(R) - kR + \tfrac{C}{k}\ln(2kR), \tag{17}$$

and thus the full phase shift reads

$$\delta_\ell - \ell\tfrac{\pi}{2} + \eta_\ell = \tilde{\theta}(\infty) - \theta(0), \tag{18}$$

which is the general form of Eq. (12).

In the Coulomb case, an integral representation can only be written if we divide the radial domain in two intervals. Indeed, unlike the previous section, $\tilde{\theta}$ now diverges logarithmically when $R \to 0$. Thus, we shall employ $\theta(R)$ for $R \le R_0$ and $\tilde{\theta}(R)$ for $R \ge R_0$, with R_0 fixed arbitrarily. Specifically, we have

$$\begin{aligned}\theta(R_0) - \theta(0) &= k\int_0^{R_0}\frac{dr}{\rho(r)} \\ \tilde{\theta}(\infty) - \tilde{\theta}(R_0) &= k\int_{R_0}^\infty dr\left[\frac{1}{\rho(r)} - 1 + \frac{C}{k^2 r}\right].\end{aligned}$$

Adding the two equations above, and making use of Eq. (17) at $R = R_0$, we find

$$\begin{aligned}\delta_\ell - \ell\tfrac{\pi}{2} + \eta_\ell &= \tilde{\theta}(\infty) - \theta(0) \\ &= k\int_0^{R_0} dr\left[\frac{1}{\rho(r)} - 1\right] + \tfrac{C}{k}\ln(2kR_0) \\ &\quad + k\int_{R_0}^\infty dr\left[\frac{1}{\rho(r)} - 1 + \frac{C}{k^2 r}\right],\end{aligned} \tag{19}$$

which represents the generalization of Eq. (13). Indeed, in the absence of the Coulomb term, i.e., setting $C = 0$ in the equations above, we have $\eta_\ell = 0$, and we recover the results of Sec. II A. We emphasize that the expression in Eq. (19) is independent of R_0, which we illustrate with numerical results in Sec. IV A. Finally, we remark that Eqs. (13, 19) yield the true value of δ_ℓ unambiguously (not modulo π), and in the case of a purely Coulombic potential, Eq. (19) yields the true value of η_ℓ.

C. Envelope and phase functions

In order to use the approach outlined above in numerical applications, it is necessary to devise a reliable method for computing the envelope directly, rather than using Eq. (6). As shown in App. B, ρ obeys a linear differential equation,

$$\rho''' - 4U\rho' - 2U'\rho = 0. \tag{20}$$

Therefore, we now regard the envelope $\rho = f^2 + g^2$ in Eq. (6) as a particular solution of Eq. (20). Namely, we impose the asymptotic boundary condition $\rho(R) \to 1$, which makes the solution unique. As we shall see in Sec. III, we initialize the envelope at $R = \infty$ and we propagate it inward; accordingly, we also propagate the reduced phase $\tilde{\theta}$ inward from $R = \infty$.

Recall that Eq. (7) allows for an integration constant to be chosen freely when constructing the phase $\theta(R)$ or $\tilde{\theta}(R)$. The integration constant can be fixed, e.g., by setting the value of $\theta(0)$, or the value of $\tilde{\theta}(\infty)$. We prefer the latter, which is suitable when employing the inward propagation mentioned above; specifically, we choose

$$\tilde{\theta}(\infty) = 0,$$

and thus Eq. (12) reads

$$\delta_\ell = \ell\tfrac{\pi}{2} - \theta(0). \tag{21}$$

The reduced phase is constructed by direct integration; in the absence of a Coulomb interaction term, we have

$$\tilde{\theta}(R) = k\int_R^\infty dr\,\frac{\tilde{\rho}(r)}{\rho(r)}, \tag{22}$$

where $\tilde{\rho}$ denotes the reduced envelope

$$\tilde{\rho} \equiv \rho - 1.$$

In the Coulomb case we make use of $\tilde{\theta}'(r) = \frac{k}{\rho(r)} - k + \frac{C}{kr}$, see Eqs. (7, 17), and thus the reduced phase reads

$$\tilde{\theta}(R) = k\int_R^\infty dr\,\left[1 - \frac{1}{\rho(r)} - \frac{C}{k^2 r}\right]. \tag{23}$$

In order to show that the integral above is well defined and yields a reduced phase obeying $\tilde{\theta}(\infty) = 0$, and also to justify that the full phase $\theta(R)$ has the asymptotic behavior (16), we write the envelope as an asymptotic series,

$$\rho(R) = 1 + \sum_{n\geq 1}\frac{b_n}{R^n}. \tag{24}$$

Assuming the potential has the long-range behavior

$$V(R) = \sum_{n\geq 1}\frac{C_n}{R^n}, \qquad \text{with } C_1 = C = \mu Z_1 Z_2,$$

we substitute the ansatz (24) in Eq. (20), and we obtain the coefficients b_n. In particular, for $n = 1$ we have $b_1 = C/k^2$, and thus the asymptotic behavior of the envelope reads

$$\rho(R) \approx 1 + \frac{C}{k^2 R} + \frac{b_2}{R^2} + \cdots.$$

Substituting the result above in Eq. (7) yields $\theta' \approx k - \frac{C}{kR} + \mathcal{O}(\frac{1}{R^2})$, which upon integration confirms Eq. (16), while the reduced phase in Eq. (23) has the asymptotic behavior

$$\tilde{\theta}(R) \approx \frac{\tilde{b}_1}{R} + \frac{\tilde{b}_2}{R^2} + \cdots \xrightarrow{R\to\infty} 0,$$

where the coefficients $\tilde{b}_n$ are expressed in terms of b_n, e.g., $\tilde{b}_1 = b_2 - b_1^2$.

For computational purposes, it is advantageous to employ the reduced envelope

$$\tilde{\rho} \equiv \rho - 1 - \tfrac{C}{k^2 r}. \tag{25}$$

Thus, we recast Eq. (23) in terms of $\tilde{\rho}$,

$$\tilde{\theta}(R) = k\int_R^\infty dr\,\frac{1}{\rho(r)}\left[\left(1 - \tfrac{C}{k^2 r}\right)\tilde{\rho}(r) - \left(\tfrac{C}{k^2 r}\right)^2\right]. \tag{26}$$

The full phase shift in Eq. (19) can now be expressed in a form suitable for computation,

$$\begin{aligned}\delta_\ell - \ell\tfrac{\pi}{2} + \eta_\ell &= -\theta(0)\\ &= k\int_0^{R_0}\frac{dr}{\rho(r)} - kR_0 + \tfrac{C}{k}\ln(2kR_0) - \tilde{\theta}(R_0).\end{aligned} \tag{27}$$

We emphasize that $\tilde{\theta}$ should be computed using Eq. (26), because the integrand in Eq. (23) suffers from cancellation at large r. Thus, in the asymptotic region, $\tilde{\rho}$ should be obtained directly, rather than ρ itself; namely, we substitute $\rho = \tilde{\rho} + 1 + C/k^2 R$ in Eq. (20) which becomes an equation for $\tilde{\rho}$. The numerical approach for solving the envelope equation is described in Sec. III, where we show that the entire asymptotic region can be treated in a numerically exact fashion by mapping it onto a finite interval and using a spectral Chebyshev method.

D. Two-envelope formula for phase shifts

We now derive a formula involving two scattering potentials; if one of them is used as a reference case, this two-envelope integral representation makes it possible to compute the phase shift δ_ℓ directly. Recall that the simple integral representations (13) and (19) yield the *full* phase shift (including Bessel and Coulomb contributions). As shown in Sec. IV B, accurate values of δ_ℓ at high ℓ cannot be obtained using Eq. (13). Thus, in this section we formulate a two-envelope approach which can be used to compute accurate phase shifts for all partial waves. For the sake of generality, we consider two different potentials V_1 and V_2, each containing the same Coulomb interaction term (if present). For a given scattering energy, $E > 0$, and a partial wave ℓ, we make use of Eq. (18) for each potential, and we employ the convenient choice $\tilde{\theta}_1(\infty) = \tilde{\theta}_2(\infty)$ to find

$$\delta_\ell^{(2)} - \delta_\ell^{(1)} = \theta_1(0) - \theta_2(0), \tag{28}$$

Using $\theta'_{1,2} = k/\rho_{1,2}$, see Eq. (7), the phase difference above can be recast as an integral,

$$\delta_\ell^{(2)} - \delta_\ell^{(1)} = k\int_0^\infty dr\Big[\frac{1}{\rho_2(r)} - \frac{1}{\rho_1(r)}\Big]. \tag{29}$$

Although both $\theta_{1,2}(R)$ diverge when $R \to \infty$, the integral above is finite because the phase difference $\theta_1(R) - \theta_2(R) = \tilde{\theta}_1(R) - \tilde{\theta}_2(R)$ vanishes asymptotically. Note that in the asymptotic region we have $\rho_1 \approx \rho_2$, which can also hold in the inner region if $V_1 \approx V_2$. Thus, Eq. (29) will suffer from catastrophic cancellation, rendering it unsuitable for numerical applications. Nevertheless, we show next that a computationally robust integral representation based on the two-envelope approach can be formulated.

We choose $V_1 \equiv V_{\rm ref}$ as a reference potential (with the corresponding effective potential including both the centrifugal and Coulomb terms, see below), while $V_2 \equiv V = V_{\rm ref} + \hat{V}$ is the full interaction potential. The reduced envelope and phase are now defined relative to the corresponding reference quantities,

$$\begin{aligned}\hat{\rho} &= \rho - \rho_{\rm ref}\\ \hat{\theta} &= \theta - \theta_{\rm ref}.\end{aligned} \tag{30}$$

We employ a nontrivial reference problem by setting

$$U_{\rm ref}(R) = -k^2 + \frac{\ell(\ell+1)}{R^2} + \frac{2C}{R}, \qquad C = \mu Z_1 Z_2, \tag{31}$$

and we use of Eqs. (28, 29) with $U_1 = U_{\rm ref}$ given above and $U_2 = U = U_{\rm ref} + 2\mu\hat{V}$. Thus, the Bessel phase shift $(-\ell\frac{\pi}{2})$ and the Coulomb phase shift η_ℓ are both eliminated, and the phase shift δ_ℓ reads

$$\begin{aligned}\delta_\ell &= -\hat{\theta}(0)\\ &= -k\int_0^\infty dr \frac{\hat{\rho}(r)}{\rho(r)\rho_{\rm ref}(r)}.\end{aligned} \tag{32}$$

The reference envelope is the solution of Eq. (20),

$$\rho'''_{\rm ref} - 4U_{\rm ref}\rho'_{\rm ref} - 2U'_{\rm ref}\rho_{\rm ref} = 0, \tag{33}$$

with $U_{\rm ref}(R)$ given in Eq. (31), while the reduced envelope obeys a non-homogeneous differential equation,

$$\hat{\rho}''' - 4U\hat{\rho}' - 2U'\hat{\rho} = 4\hat{U}\rho'_{\rm ref} + 2\hat{U}'\rho_{\rm ref}, \tag{34}$$

which was obtained by combining Eqs. (20) and (33). In the equation above we used the notation $\hat{U} \equiv U - U_{\rm ref} = 2\mu\hat{V}$. Note that in the absence of a Coulomb term, we use $U_{\rm ref} = -k^2 + \frac{\ell(\ell+1)}{R^2}$, with $V_{\rm ref} = 0$ and $\hat{V} = V$, which is illustrated with numerical results in Sec. IV B. Finally, we remark that in the absence of a Coulomb term one can also use the trivial choice $U_{\rm ref} = -k^2$ with $\theta_{\rm ref}(R) = kR$, which yields $\hat{\theta}$ identical to $\tilde{\theta}$ in Eq. (11), thus recovering the integral representation of the full phase shift given in Sec. II A.

In practical applications, one first solves Eq. (33) for the reference envelope, which is subsequently used in Eq. (34). The latter is solved to obtain $\hat{\rho}$, and thus the full envelope is obtained: $\rho = \rho_{\rm ref} + \hat{\rho}$. We remark that the numerical approach used for the homogeneous envelope equation, see Sec. III, can also be employed for the non-homogeneous differential equation (34). The two-envelope approach is fully general, but is especially useful when $\hat{U} = 2\mu\hat{V}$ is small, such that $|\hat{\rho}| \ll \rho \approx \rho_{\rm ref}$, and thus $\hat{\theta}$ and δ_ℓ will also be small.

III. COMPUTATIONAL APPROACH

The integral representations derived in this article are valid in general; however, they are useful in numerical applications only if the integrands are well behaved. Specifically, the envelope should behave in a non-oscillatory fashion, which in turn ensures the smoothness of the phase function. In practice, there is considerable difficulty in finding the smooth envelope [4, 45], because the general solution of the envelope equation has an oscillatory behavior, as mentioned in App. A. In this section, a novel computational strategy for obtaining the *smooth* envelope in the asymptotic region is presented. We emphasize that finding the unique, smooth solution is critically important for the efficiency and accuracy of numerical schemes using our integral representations, and for using the phase–amplitude method in general.

For clarity, we assume that $V(R)$ vanishes faster than R^{-1} asymptotically. As discussed in Sec. II A (see also App. C), we employ the initial condition $\rho = 1$ at $R = \infty$ when solving Eq. (20). However, rather than using the radial variable, it is highly advantageous to reformulate the envelope equation by *mapping* the asymptotic radial domain onto a finite interval. We developed a convenient and efficient numerical implementation based on a simple change of variable,

$$x = \frac{1}{R},$$

which allows to take fully into account the long-range tail of any potential. Thus, the *infinite* radial interval $R_1 < R < \infty$ is now mapped on a compact interval, $x_1 > x > 0$, with $x_1 = \frac{1}{R_1}$. The boundary R_1, i.e., the size of the interval $[0,\, x_1]$, will be chosen to ensure the desired level of accuracy.

We now regard the envelope as an x-dependent function, and we present the computational approach for finding the smooth solution of the envelope equation inside the interval $[0,\, x_1]$. First, we rewrite Eq. (20) using $x = \frac{1}{R}$ as the independent variable,

$$x^4\dddot{\rho} + 6x^3\ddot{\rho} + 6x^2\dot{\rho} - 4U\dot{\rho} - 2\dot{U}\rho = 0, \tag{35}$$

where dots above symbols denote derivatives with respect to x, e.g., $\dot{\rho} = d\rho/dx$. Recall that $U = 2\mu V_{\rm eff} - k^2$. Next, we define

$$u \equiv \dot{\rho},$$

and we regard it as the unknown function. Making use of the initial condition $\rho = 1$ at $x = 0$, we write

$$\rho(x) = 1 + \int_0^x dt\, u(t),$$

which we substitute in the last term of Eq. (35) to obtain

$$\left(4k^2 - 8\mu V_{\rm eff} + x^4 D_x^2 + 6x^3 D_x + 6x^2 - 4\mu \dot{V}_{\rm eff} S_x\right) u = 4\mu \dot{V}_{\rm eff}. \tag{36}$$

The operators D_x and S_x read

$$D_x u = \dot{u} = \frac{du}{dx}, \qquad S_x u = \int_0^x dt\, u(t).$$

We solve Eq. (36) using a spectral Chebyshev method [46–51], i.e., we employ a small number of Chebyshev polynomials $T_n(x)$ with $n = 0, 1, 2, \ldots, N-1$, which are mapped onto the interval $[0, x_1]$. We expand the unknown function $u(x)$ in the Chebyshev basis, and the operators D_x and S_x are represented as finite $(N \times N)$ matrices [48, 49]. Thus, Eq. (36) becomes a simple linear system,

$$\mathbf{MA} = \mathbf{B}, \tag{37}$$

where the column $\mathbf{A}$ contains the Chebyshev coefficients of our unknown function,

$$u(x) = \sum_{n=0}^{N-1} A_n T_n(x),$$

$\mathbf{B}$ contains the Chebyshev coefficients for the expansion

$$4\mu \dot{V}_{\rm eff}(x) = \sum_{n=0}^{N-1} B_n T_n(x),$$

and $\mathbf{M}$ is the matrix of the operator in Eq. (36),

$$M = 4k^2 - 8\mu V_{\rm eff} + x^4 D_x^2 + 6x^3 D_x + 6x^2 - 4\mu \dot{V}_{\rm eff} S_x.$$

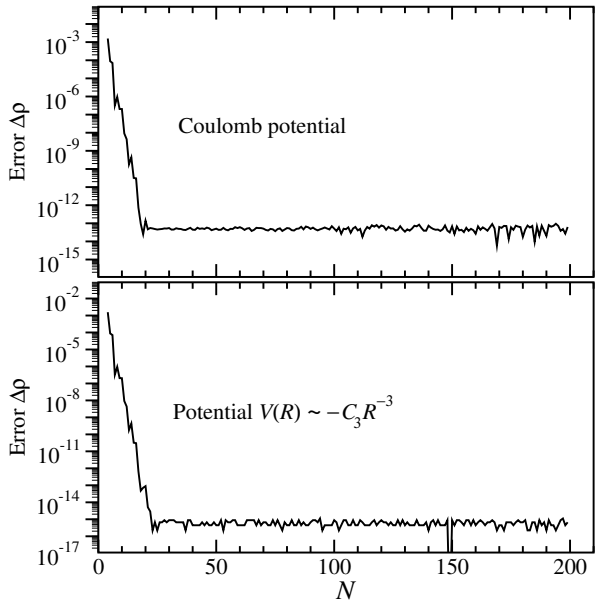

FIG. 1. Upper: convergence test for an attractive Coulomb potential with $C = -1$, for $\ell = 5$ and $k = 0.1$ a.u. The horizontal axis is the size N of the Chebyshev basis, while the the vertical axis is the error for the envelope. Lower: same as the upper panel, for the potential $V(R)$ given in Eq. (40), for $\ell = 475$ and $E = 0.002$ a.u.

Although the operator M is singular, its associated matrix ($\mathbf{M}$) in the finite Chebyshev basis is well conditioned and yields highly accurate solutions; indeed, the matrix $\mathbf{M}$ does admit an inverse, and the solution of Eq. (37) reads $\mathbf{A} = \mathbf{M}^{-1}\mathbf{B}$. Figure 1 depicts the error $\Delta\rho = \left|\rho^{(N)}(x_1) - \rho^{(N_{\rm max})}(x_1)\right|$ for the envelope evaluated at $x_1 = 0.04$. We varied the size of the Chebyshev basis from $N = 5$ to $N_{\rm max} = 200$, as shown in Fig. 1, which makes it readily apparent that the convergence with respect to N is robust. The smooth envelope is thus obtained as the unique solution; indeed, all the other solutions oscillate infinitely fast near $x = 0$ ($R \to \infty$) and they are eliminated simply because highly oscillatory behavior cannot be accommodated by the finite number of polynomials.

We emphasize that the linearity of the envelope equation is crucially important for the feasibility of the approach presented here. Finally, the solution obtained inside the interval $[0, x_1]$ can now be used to initialize the propagation for $x > x_1$, i.e., $R < R_1$. A detailed description of our computational approach will be published elsewhere.

The advantage of the phase–amplitude method combined with the change of variable $x = \frac{1}{R}$ is readily apparent in Fig. 2, where we show the x-dependence of the reduced phase $\tilde{\theta}(x)$ and the envelope $\rho(x)$ along with $|\psi|^2$ for $\ell = 475$ and

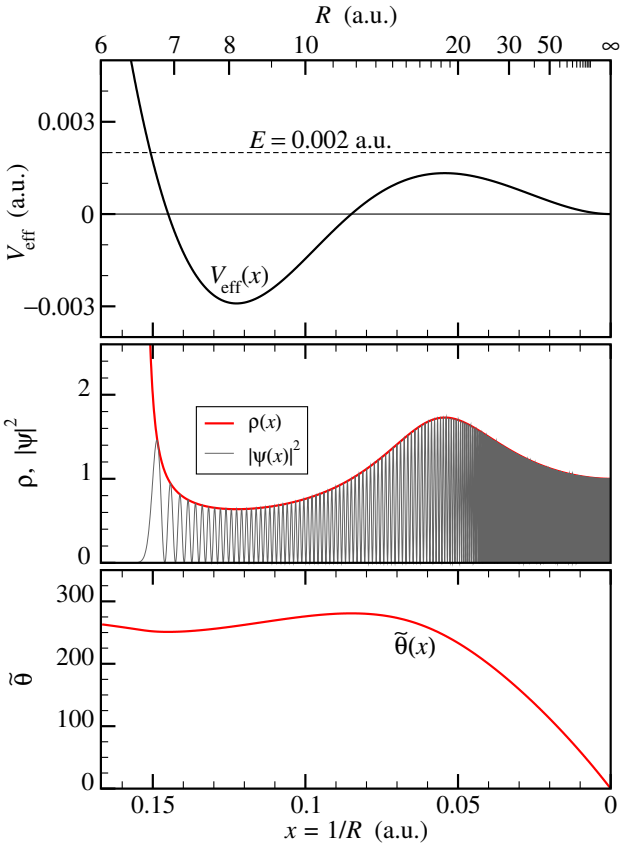

FIG. 2. Upper: effective potential (for $\ell = 475$) as a function of $x = \frac{1}{R}$. $V(R)$ is given in Eq. (40). The values of R are indicated at the top. The horizontal dashed line marks the energy E. Middle: thin line (gray) for the wave function, thick line (red) for the envelope. Lower: reduced phase $\tilde{\theta}(x)$.

$E = 0.002$ a.u., for the potential energy used in Sec. IV B, see Eq. (40). Note that the wave function in Fig. 2 was evaluated numerically using Eq. (8), i.e., $\psi = \sqrt{\rho}\sin(\theta - \theta_{R=0})$.

When the potential has a repulsive wall at short range, the formulation of the phase–amplitude approach based on the change of variable $x = \frac{1}{R}$ can be employed for the entire radial domain, as shown in Fig. 2. Indeed, the repulsive wall makes it possible to stop the inward propagation at $R_{\rm min} > 0$, which corresponds to a finite value $x_{\rm max} = \frac{1}{R_{\rm min}}$. We remark that, when the inward propagation of the reduced phase $\tilde{\theta}$ approaches the repulsive wall, it is convenient to convert it to the full phase θ using Eq. (11) at a point R_0 just outside the inner wall; for the remainder of the radial domain ($R < R_0$), one should propagate $\theta(R)$ instead of $\tilde{\theta}(R)$, because the former converges much faster than the latter. Indeed, if $V_{\rm eff} \to +\infty$ when $R \to 0$, we have $\rho \to \infty$ and $\theta' \to 0$, while $\tilde{\theta}' \to -k$. In other words, $\theta(0)$ should be computed as

$$\theta(0) = kR_0 + k\int_{R_0}^{\infty} dr\,\frac{\tilde{\rho}(r)}{\rho(r)} - k\int_{R_{\rm min}}^{R_0}\frac{dr}{\rho(r)}, \qquad (38)$$

which is independent of R_0. We remark that the integration need not extend fully to $R = 0$, because $R_{\rm min}$ is chosen inside the repulsive wall to ensure the contribution of the interval $0 < R < R_{\rm min}$ is entirely negligible. Consequently, the radial domain can be safely restricted to $R_{\rm min} < R < \infty$, which is mapped onto the compact interval $x_{\rm max} > x > 0$.

IV. EXAMPLES

We now apply the integral representations and show that they yield highly accurate results. Our first example is the Coulomb potential, which we use as a test case for the integral representation (27). The two-envelope formula, see Eqs. (28) and (32), will be employed and tested in Sec. IV B.

A. The Coulomb potential

In the case of a purely Coulombic potential, Eq. (27) yields the Coulomb phase shift,

$$\eta_\ell = \ell\tfrac{\pi}{2} - kR_0 + \tfrac{C}{k}\ln(2kR_0) + k\int_0^{R_0}\frac{dr}{\rho(r)} - \tilde{\theta}(R_0), \qquad (39)$$

with $\tilde{\theta}$ given Eq. (26). The result above is independent of R_0, as depicted in Fig. 3. Indeed, we show that our approach is robust and accurate by comparing the value of η_ℓ obtained using Eq. (39) with the exact value $\eta_\ell^\Gamma \equiv \arg\Gamma(\ell + 1 + i\frac{C}{k})$ for $C = -1$, $k = 0.1$ and $\ell = 5$. Our integral representation yields the value $\eta_\ell = -20.22421961527$, while the analytical expression gives its value modulo 2π, namely $\eta_\ell^\Gamma = -1.3746636937335435$. Their difference equals an integer multiple of 2π to a high degree of precision: $(\eta_\ell - \eta_\ell^\Gamma)/2\pi = -3(1 \pm 10^{-13})$. Figure 3 depicts the relative error $|(\eta_\ell - \eta_\ell^\Gamma + 6\pi)/\eta_\ell|$ as a function of R_0.

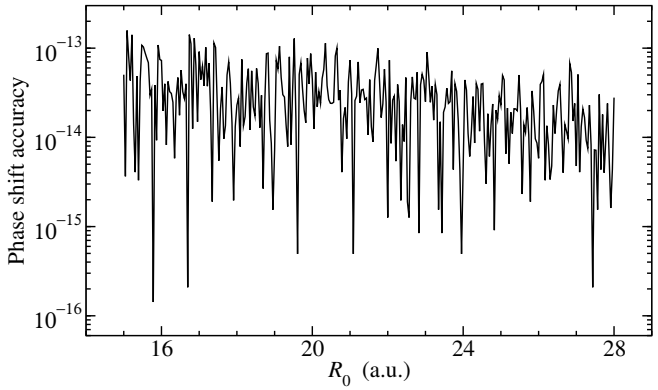

FIG. 3. Relative error of the computed Coulomb phase shift η_ℓ for $C = -1$, $k = 0.1$ and $\ell = 5$. Equation (39) yields a highly accurate result that is independent of R_0.

B. Results for an inter-atomic potential with long-range behavior of the type $V(R) \sim -\frac{C_3}{R^3}$

For our second example we use both integral representations, i.e., Eq. (13) for the full phase shift and the two-envelope formula (32) which yields the phase shift directly. We employ the potential energy

$$V(R) = C_{\rm wall}\exp\left(-\frac{R}{R_{\rm wall}}\right) - \frac{C_3}{R^3 + R_{\rm core}^3}, \qquad (40)$$

with $C_{\rm wall} = 10$, $R_{\rm wall} = 1$, $R_{\rm core} = 5$ and $C_3 = 18$ (all in atomic units), and the reduced mass $\mu = \frac{m}{2}$, where m is the mass of ^{88}Sr. We computed phase shifts for $E = 0.01$ a.u. ≈ 0.272 eV for a wide range of partial waves. The upper panel in Fig. 4 depicts the ℓ dependence of the phase shift, while the lower panel shows the partial-wave terms of the elastic cross section, $\sigma_\ell = \frac{4\pi}{k^2}(2\ell+1)\sin^2\delta_\ell$. An exceedingly large number of partial waves contribute to the cross section; note that the dominant contribution stems from very high partial waves ($\ell > 5000$). For a fully converged value of the elastic cross section, we have computed phase shifts up to $\ell = 10^5$.

Recall that our integral representations yield the true value of the phase shift (not modulo π) which has a rather simple ℓ-dependence; this suggests that interpolation schemes could be used to drastically reduce the number of partial waves for which phase shifts need to be computed. This added advantage is illustrated in Fig. 5, where we compare the true phase shift with its modulo π version. Moreover, our approach is not restricted to integer values of ℓ, and makes it possible to use non-integer values of ℓ as interpolation points; thus, highly accurate interpolation methods with non-uniform grids, e.g., Chebyshev interpolation, can be employed.

Regarding the practical aspects of the computation, some remarks are in order. We first emphasize that, using the computational approach presented in Sec. III, the simple integral representation (13) and the two-envelope formula (32) can be implemented numerically such that they both yield accurate results. However, when using the integral representation (13) for the *full* phase shift, the value of δ_ℓ obtained from Eq. (21)

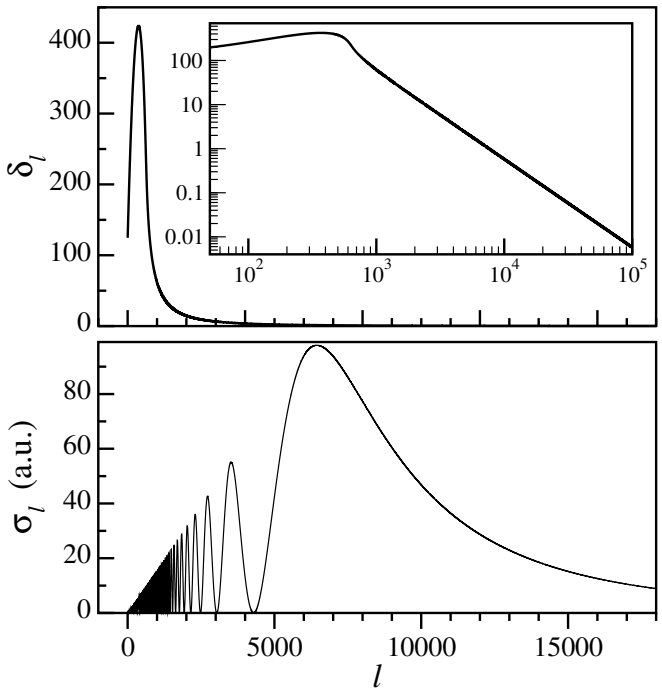

FIG. 4. Phase shifts and cross section terms $\sigma_\ell = \frac{4\pi}{k^2}(2\ell+1)\sin^2\delta_\ell$ for the potential energy in Eq. (40) for $E = 0.01$ a.u.

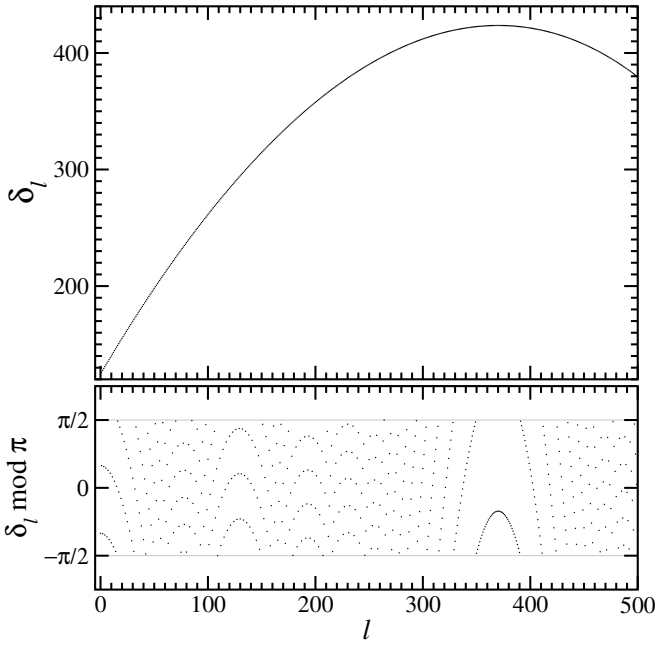

FIG. 5. Phase shift δ_ℓ corresponding to the R^{-3} potential in Eq. (40) and $E = 0.01$ a.u., for discrete integer values of ℓ. Upper: true value of δ_ℓ. Lower: $\delta_\ell \bmod \pi$. Note the vastly different scales used for the vertical axis in the two panels.

will gradually lose precision at very high ℓ. Indeed, for $\ell \to \infty$ we have $\delta_\ell \to 0$ while $\theta(0) \approx \ell\frac{\pi}{2}$. Therefore, the simple integral representation (13) must be avoided at high ℓ because of the catastrophic cancellation in Eq. (21), even though $\theta(0)$ can still be computed accurately. Consequently, when ℓ becomes extremely large, δ_ℓ should instead be computed using the two-envelope formula derived in Sec. II D.

Although the two-envelope formula is highly accurate for all partial waves, Eq. (13) has the advantage of much greater simplicity and could be used at low ℓ, provided that it is sufficiently accurate. A simple rule of thumb exists for finding the highest partial wave for which Eqs. (13, 21) yield accurate results. Namely, the two-envelope formula needs to replace the simple formula only if ℓ is high enough for the centrifugal term to become dominant over $V(R)$. We show next that the simple formula is indeed accurate at low ℓ; moreover, it is less expensive computationally compared to the two-envelope approach, which requires twice the amount of numerical work. The highest partial wave, $\ell_{\max}$, for which the simple formula is still accurate can be estimated as follows; we extract $\ell_{\max}$ by equating the depth of the potential well, $V_D = |V(R_{\text{bottom}})|$, which sets the energy scale at short range, with the centrifugal term evaluated at R_{bottom}, the location of the minimum of $V(R)$. Namely, we have $\ell_{\max}(\ell_{\max}+1) = 2\mu R_{\text{bottom}}^2 V_D$. Thus, for the potential used in our example we estimate the simple formula to maintain high accuracy for $\ell \lessapprox 460 = \ell_{\max}$, which we confirm below. Note that in the high energy limit we have $|V(R)| \ll E$, and the two-envelope formula should be used for all partial waves ℓ, because all phase shifts δ_ℓ are vanishingly small when $E \to \infty$.

We first performed a test for the Bessel case, $V_{\text{eff}} = \frac{\ell(\ell+1)}{2\mu R^2}$, with $V = 0$, in order to show that the two-envelope formula is robust and accurate even for very high ℓ. Namely, we computed directly the vanishingly small difference between the Bessel phase shifts for ℓ_1 and ℓ_2 which are nearly equal. We used $\ell_1 = \ell$ and $\ell_2 = \ell - \frac{1}{\ell^2}$, for which the exact value of $\delta_\ell = \delta_B(\ell_2) - \delta_B(\ell_1)$ is $\delta_\ell = \frac{\pi}{2\ell^2}$, where $\delta_B(\ell) = -\ell\frac{\pi}{2}$ denotes the Bessel phase shift. The relative error of the numerical value δ_ℓ obtained with the two-envelope formula is shown in Fig. 6, confirming that high accuracy is preserved at high ℓ, despite the smallness of δ_ℓ. In contrast, if the *exact* values of $\delta_B(\ell_{1,2})$ are subtracted numerically, the loss of accuracy is significant and becomes catastrophic at very high ℓ, see Fig. 6. This also illustrates that the failure of Eq. (21) at high ℓ cannot be avoided, as it is due to the cancellation of nearly equal quantities. Nevertheless, Eq. (21) is sufficiently accurate at low ℓ. Indeed, we performed a test for the simple integral representation (13). Assuming the two-envelope formula is numerically exact, the relative error for δ_ℓ computed using Eqs. (13, 21) for the nontrivial potential energy (40) is shown in Fig. 7, which makes it readily apparent that the simple formula is highly accurate for partial waves $\ell \lessapprox 460$, while significant loss of precision only occurs for much higher ℓ.

V. CONCLUSIONS AND FUTURE WORK

In this work we presented a novel integral representation for scattering phase shifts. A simple version, Eq. (13), yields the so called full phase shift, while the two-envelope formula can be used to obtain δ_ℓ directly. We emphasize that, unlike

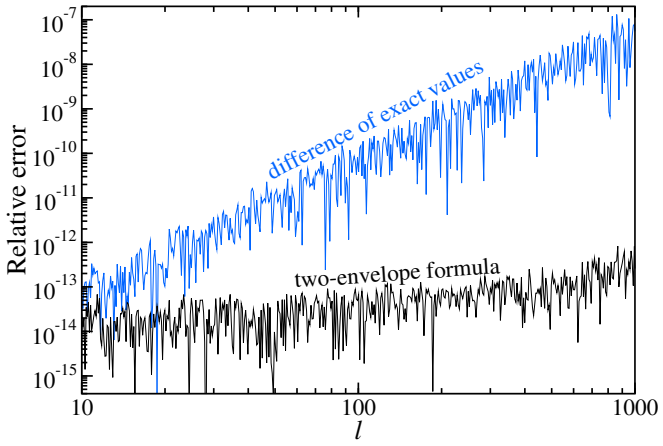

FIG. 6. Relative error for the Bessel test. Blue line for the difference of the exact Bessel phase shifts, see text; black line for the two-envelope formula.

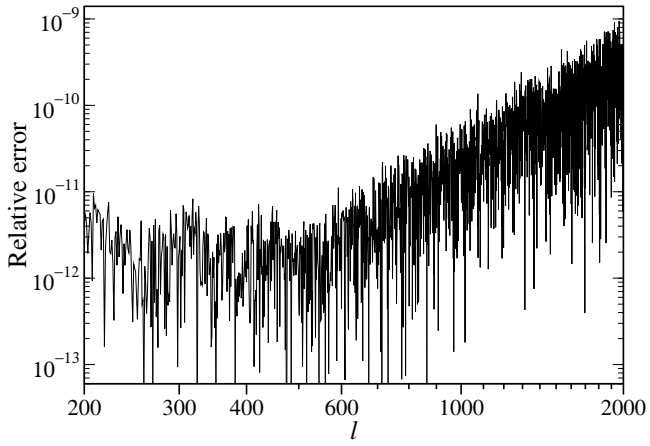

FIG. 7. Comparison of the simple integral representation (13) and the two-envelope formula (32). The simple integral representation is highly accurate for $\ell \lessapprox 460$, and then gradually loses accuracy for higher ℓ.

standard approaches which only yield $\delta_\ell \bmod \pi$, our integral representations give the true value of the phase shift. The integral representations are very useful in numerical applications, as shown in Sec. IV; indeed, they can be easily implemented to obtain highly accurate results. Moreover, our approach is based on the phase–amplitude method, which avoids the explicit computation of highly oscillatory wave functions; thus, our numerical implementations are very efficient, and are consistently accurate even for very high partial waves.

We remark that our integral representations are always valid, but the computational advantages mentioned above rely on the assumption that the envelope is globally smooth. However, a globally smooth solution of the envelope equation (20) does not always exist; indeed, as is well known [15], when a barrier separates two classically allowed regions, the solution which is smooth on one side of the barrier will oscillate on the other side. To overcome this computational difficulty, it is necessary to develop an optimization procedure for finding the locally smooth envelopes. In addition, one needs to find a way to combine the different solutions which are locally optimized in each classically allowed region. This is a nontrivial task, as it requires certain functional relationships be established between the envelopes and phases corresponding to disjoint regions which are separated by a barrier. If such an approach could be rendered computationally feasible, it would yield the true phase-shift even in the absence of a globally smooth envelope.

ACKNOWLEDGMENTS

This work was partially supported by the National Science Foundation Grant No. PHY-1415560 (DS), and MURI Army Research Office Grant No. W911NF-14-1-0378 (IS, RC).

Appendix A: The phase–amplitude approach

A brief overview of Milne's phase–amplitude approach is presented here. According to Milne [1], the *general* solution ψ of the radial equation (1) can be expressed in terms of an amplitude y and a phase θ,

$$\psi(R) = c\, y(R) \sin[\theta(R) + \theta_0], \tag{A1}$$

where c and θ_0 are arbitrary constants. The amplitude satisfies the nonlinear equation

$$y'' = Uy + \frac{q^2}{y^3}, \tag{A2}$$

with $U = 2\mu(V_{\text{eff}} - E)$, and the phase $\theta(R)$ is constructed by integrating

$$\theta' = \frac{q}{y^2}. \tag{A3}$$

In the equations above, q is arbitrary; the only restriction is $q^2 > 0$ in the amplitude equation (A2). We emphasize that the amplitude and phase appearing in Milne's parametrization (A1) are not unique; indeed, any solution y of Eq. (A2) together with the associated phase θ will give a valid representation of ψ. This undermines the advantage of Milne's method in numerical applications, because the general solution $y(R)$ of Milne's nonlinear equation has an oscillatory behavior in classically allowed regions, and the unique smooth amplitude is very difficult to find [4, 45, 52]. Despite this difficulty, Milne's nonlinear equation (A2) has long been used for computational work. We remark that an *equivalent* formulation based on a *linear* equation exists [53, 54], but it remained overlooked in the physics community until recently [55]. As we show in App. B, the linear equation can be obtained by simply replacing the amplitude with the *envelope* function ρ,

$$\rho(R) = y^2(R). \tag{A4}$$

The envelope obeys a third order linear differential equation,

$$\rho''' = 4U\rho' + 2U'\rho. \tag{A5}$$

In App. B we present two different derivations for the envelope equation (A5), and in App. C we discuss its equivalence with Milne's nonlinear equation (A2).

Although Eq. (A5) is of third order, its linearity makes it much more convenient than Milne's nonlinear equation (A2). However, finding the non-oscillatory solution is still a difficult task. To overcome this obstacle, we devised a computational strategy for scattering problems ($E > 0$) which yields the smooth envelope in the asymptotic region, see Sec. III.

Appendix B: The envelope equation

We present here two different derivations of the envelope equation (20, A5). The first derivation is very brief; namely, we substitute $y = \sqrt{\rho}$ in equation (A2) and we find

$$\rho'' = 2U\rho + \frac{1}{\rho}\left[\tfrac{1}{2}(\rho')^2 + 2q^2\right].$$

Next, we multiply both sides by ρ to obtain

$$\rho\rho'' = 2U\rho^2 + \frac{1}{2}(\rho')^2 + 2q^2, \tag{B1}$$

which is still a nonlinear equation. However, we now take the derivatives of both sides,

$$\rho\rho''' = 4U\rho\rho' + 2U'\rho^2,$$

and we divide by ρ to finally obtain Eq. (A5).

The second approach is similar to Milne's derivation [1] of Eq. (A2). Namely, we consider two solutions (ϕ and χ) of the radial Schrödinger equation (1), and we try to find a differential equation for their product

$$p \equiv \phi\chi.$$

Making use of Eq. (1) for ϕ and χ, we obtain

$$p'' = 2Up + 2\phi'\chi',$$

and we now evaluate its derivative,

$$p''' = 2U'p + 2Up' + 2U(\phi\chi' + \phi'\chi),$$

where we recognize $p' = \phi\chi' + \phi'\chi$, and we find again the envelope equation (A5),

$$p''' = 4Up' + 2U'p.$$

As the product of *any* two solutions of the radial equation obeys the envelope equation, ϕ^2 and χ^2 are also valid solutions of Eq. (A5), as well as any linear combination of ϕ^2, χ^2 and $\phi\chi$ [7, 56]. In particular, $\rho = \phi^2 + \chi^2$ is a valid solution, which corresponds to Milne's ansatz $y = \sqrt{\phi^2 + \chi^2}$.

Appendix C: Milne's amplitude equation as a constraint for the envelope equation

The parameter q appears explicitly in Milne's nonlinear equation (A2). However, q is absent from the envelope equation (A5), even though it is used when integrating Eq. (7) to obtain the phase θ. This creates some ambiguity, which stems from the fact Eq. (A2) is a second order differential equation, while the Eq. (20) is of third order. We now try to dispel the ambiguity and show that the two equations are equivalent. We first remark that although q does not appear in Eq. (20), it should be assumed implicitly; indeed, if we recast Eq. (B1) in the form

$$\frac{1}{2}\rho\rho'' - U\rho^2 - \frac{1}{4}(\rho')^2 = q^2, \tag{C1}$$

the expression on the left hand side can be interpreted as an invariant of the envelope equation (A5), and any solution ρ will also obey Eq. (C1) with a particular value of q^2. Recall that the equation above is equivalent with Milne's equation (A2), which can thus be regarded as a constraint for the envelope equation. Indeed, as we discuss below, Eq. (C1) should be used to enforce the correct initial conditions for ρ, such that they correspond to a fixed value for q.

To fully clarify the equivalence of Eqs. (A2) and (A5), let us compare the sets of initial conditions required in each case. When we initialize ρ at $R = R_0$, we consider given

$$\rho(R_0), \qquad \rho'(R_0), \qquad \rho''(R_0),$$

which can be used in the constraint equation (C1) evaluated at $R = R_0$ to obtain the value of q. Conversely, if q is considered given, we have

$$\rho(R_0), \qquad \rho'(R_0), \qquad q = \text{fixed},$$

which we commonly employ in practice. Equation (C1) is now used to obtain $\rho''(R_0)$, and thus initialize the solution of the envelope equation. Equivalently, for Milne's amplitude equation we consider given

$$y(R_0), \qquad y'(R_0), \qquad q = \text{fixed}.$$

Moreover, the families of solutions for different values of q are all equivalent. Indeed, if y_1 is a solution of Eq. (A2) for a given parameter q_1, then $y_2 = (q_2/q_1)^{\frac{1}{2}} y_1$ is a solution for q_2. Similarly, we have $\rho_2/q_2 = \rho_1/q_1$, and $\theta_2' = \theta_1'$. Varying the parameter q is entirely redundant, as the phase θ remains unchanged, therefore justifying the convenient choice $q = k$ used throughout this article.

Finally, we make use of the constraint in Eq. (C1) to show that the choice $q = k$ is consistent with the initial condition $\rho = 1$ at $R = \infty$, which gives a convenient normalization for the envelope. Indeed, when $R \to \infty$, we have $V_{\text{eff}}(R) \to 0$ and thus $U(R) \approx U(\infty) = -k^2$ and $U' \approx 0$, while for the envelope we have

$$\rho(R) \approx \rho(\infty), \qquad \rho'(R) \approx 0, \qquad \rho''(R) \approx 0.$$

Substituting these asymptotic values in Eq. (C1) we obtain

$$-U(\infty)\rho^2(\infty) = q^2,$$

and using $U(\infty) = -k^2$, we find the parameter q,

$$q = k\rho(\infty).$$

Conversely, if one prefers to choose a certain value for q, the equation above yields $\rho(\infty) = q/k$. However, as shown above, the normalization constant $\rho(\infty)$ is irrelevant; indeed, we have

$$\theta'(R) = \frac{q}{\rho(R)} = k\frac{\rho(\infty)}{\rho(R)},$$

which ensures

$$\theta'(R) \approx k, \qquad \text{when } R \to \infty,$$

and thus the phase function suitable for scattering problems, as defined in Sec. II A, has the desired behavior:

$$\theta(R) \approx kR, \qquad \text{when } R \to \infty.$$

[1] W. E. Milne, Phys. Rev. **35**, 863 (1930).
[2] J. L. Bohn, Phys. Rev. A **49**, 3761 (1994).
[3] J. L. Bohn and P. S. Julienne, Phys. Rev. A **60**, 414 (1999).
[4] F. Robicheaux, U. Fano, M. Cavagnero, and D. A. Harmin, Phys. Rev. A **35**, 3619 (1987).
[5] C. Jungen, F. Texier, and C. Jungen, J. Phys. B **33**, 2495 (2000).
[6] J. P. Burke, C. H. Greene, and J. L. Bohn, Phys. Rev. Lett. **81**, 3355 (1998).
[7] B. Yoo and C. H. Greene, Phys. Rev. A **34**, 1635 (1986).
[8] C. H. Greene, A. R. P. Rau, and U. Fano, Phys. Rev. A **26**, 2441 (1982).
[9] A. Crubellier and E. Luc-Koenig, J. Phys. B **39**, 1417 (2006).
[10] L. B. Zhao, I. I. Fabrikant, J. B. Delos, F. Lépine, S. Cohen, and C. Bordas, Phys. Rev. A **85**, 053421 (2012).
[11] F. H. J. Hall, M. Aymar, M. Raoult, O. Dulieu, and S. Willitsch, Mol. Phys. **111**, 1683 (2013).
[12] M. Raoult and G. G. Balint-Kurti, Phys. Rev. Lett. **61**, 2538 (1988).
[13] I. Fourré and M. Raoult, J. Chem. Phys. **101**, 8709 (1994).
[14] J. M. Lecomte and M. Raoult, Mol. Phys. **105**, 1575 (2007).
[15] S.-Y. Lee and J. C. Light, Chem. Phys. Lett. **25**, 435 (1974).
[16] J.-M. Yuan and J. C. Light, Int. J. Quantum Chem. **8**, 305 (1974).
[17] J.-M. Yuan and J. C. Light, Int. J. Quantum Chem. **8**, 305 (1974).
[18] A. Bar-Shalom, M. Klapisch, and J. Oreg, J. Quant. Spectr. Rad. Transf. **71**, 169 (2001).
[19] J. Rundgren, Phys. Rev. B **76**, 195441 (2007).
[20] C. Rogers, B. Malomed, K. Chow, and H. An, J. Phys. A **43**, 455214 (2010).
[21] A. Thilagam, J. Phys. A **43**, 354004 (2010).
[22] I. A. Pedrosa, Phys. Rev. A **83**, 032108 (2011).
[23] G. Reinisch, Phys. Lett. A **372**, 769 (2008).
[24] J. E. Lidsey, Class. Quantum Grav. **21**, 777 (2004).
[25] R. M. Hawkins and J. E. Lidsey, Phys. Rev. D **66**, 023523 (2002).
[26] R. Kaushal, Class. Quantum Grav. **15**, 197 (1998).
[27] K. Bakke, I. Pedrosa, and C. Furtado, J. Math. Phys. **50**, 113521 (2009).
[28] K. V. Khmelnytskaya and H. C. Rosu, J. Phys. A **42**, 042004 (2008).
[29] F. H. Mies and M. Raoult, Phys. Rev. A **62**, 012708 (2000).
[30] R. Osséni, O. Dulieu, and M. Raoult, J. Phys. B **42**, 185202 (2009).
[31] B. Yoo and C. H. Greene, Phys. Rev. A **34**, 1635 (1986).
[32] Z. Idziaszek, A. Simoni, T. Calarco, and P. S. Julienne, New J. Phys. **13**, 083005 (2011).
[33] B. Segev, R. Côté, and M. G. Raizen, Phys. Rev. A **56**, R3350 (1997).
[34] R. Côté, B. Segev, and M. G. Raizen, Phys. Rev. A **58**, 3999 (1998).
[35] R. Côté and A. Dalgarno, J. Mol. Spectrosc. **195**, 236 (1999).
[36] Z. Pavlović, R. V. Krems, R. Côté, and H. R. Sadeghpour, Phys. Rev. A **71**, 061402 (2005).
[37] P. Zhang, A. Dalgarno, and R. Côté, Phys. Rev. A **80**, 030703 (2009).
[38] J. Stanojevic, R. Côté, D. Tong, S. M. Farooqi, E. E. Eyler, and P. L. Gould, Eur. Phys. J. D **40**, 3 (2006).
[39] J. Stanojevic, R. Côté, D. Tong, E. E. Eyler, and P. L. Gould, Phys. Rev. A **78**, 052709 (2008).
[40] N. Geum, G.-H. Jeung, A. Derevianko, R. Côté, and A. Dalgarno, J. Chem. Phys. **115**, 5984 (2001).
[41] M. Gacesa, P. Pellegrini, and R. Côté, Phys. Rev. A **78**, 010701 (2008).
[42] J. Deiglmayr, P. Pellegrini, A. Grochola, M. Repp, R. Côté, O. Dulieu, R. Wester, and M. Weidemller, New J. Phys. **11**, 055034 (2009).
[43] D. Shu, I. Simbotin, and R. Côté, ChemPhysChem **17**, 3655 (2016).
[44] M. J. Seaton, Comput. Phys. Comm. **146**, 225 (2002).
[45] E. Y. Sidky, Phys. Essays **13**, 408 (2000).
[46] C. W. Clenshaw and A. R. Curtis, Numer. Math. **2**, 197 (1960).
[47] S. E. El-gendi, Comput. J. **12**, 282 (1969).
[48] L. Greengard, SIAM J. Numer. Anal. **28**, 1071 (1991).
[49] R. Gonzales, J. Eisert, I. Koltracht, M. Neumann, and G. Rawitscher, J. Comput. Phys. **134**, 134 (1997).
[50] B. Mihaila and I. Mihaila, J. Phys. A **35**, 731 (2002).
[51] G. Rawitscher, Comput. Phys. Commun. **191**, 33 (2015).
[52] A. Matzkin, Phys. Rev. A **63**, 012103 (2000).
[53] W. K. Schief, Appl. Math. Lett. **10**, 13 (1997).
[54] S. Moyo and P. Leach, J. Math. Anal. Appl. **252**, 840 (2000).
[55] S. Kiyokawa, AIP Adv. **5**, 087150 (2015).
[56] E. Pinney, Proc. Am. Math. Soc. **1**, 681 (1950).